Stark effect in shallow impurities in Si

G. D. J. Smit, S. Rogge,* J. Caro, and T. M. Klapwijk
Kavli Institute of Nanoscience, Delft University of Technology, Lorentzweg 1, 2628 CJ Delft, The Netherlands
(Received 17 October 2003; published 21 July 2004)

We have theoretically studied the effect of an electric field on the energy levels of shallow donors and acceptors in silicon. An analysis of the electric field dependence of the lowest energy states in donors and acceptors is presented, taking the band structure into account. A description as hydrogenlike impurities was used for accurate computation of energy levels and lifetimes up to large (several MV/m) electric fields. All results are discussed in connection with atomic scale electronics and solid state quantum computation.

DOI: 10.1103/PhysRevB.70.035206 PACS number(s): 71.70.Ej, 71.55.Cn, 03.65.Fd, 03.67.Lx

I. INTRODUCTION

The field of atomic scale electronics (ASE) aims at controlling charge and spin in semiconductors at the level of *individual* dopant atoms. Such an ability is very attractive, both for physics and for the development of (quantum) devices. From a fundamental point of view, dopant atoms are interesting, because they can be considered as the solid state analog of atoms in free space. Several well-known effects from atomic physics (e.g., the Stark effect and the Zeeman effect) have been studied in great detail in large ensembles of dopant atoms.[1] The prospect of experimentally realizing atomic scale electronics has renewed the interest in dopant atoms. Measurement and control of individual dopant atoms allows for the observation of quantum coherent time evolution and interactions of the dopant's wave functions, which is essential for the operation of a quantum computer.

Manipulation of a single particle's wave functions can be realized by using a local magnetic or electric field. Such a field can be used either to perform the desired manipulation itself, or to provide a local perturbation allowing for addressing a single impurity by a global radiation field. A local electric field could be realized by putting a small gate close to a dopant atom, which is in principle accomplishable with current technology. An ultimate application of gate manipulation is found in the solid state quantum computer as proposed by Kane.[2,3]

To get more insight into the physics of atomic scale electronic devices, it is essential to try to predict their potential behavior. A first step is the description of isolated dopant atoms in a (homogeneous) electric field. Much more difficult is accurate modeling of the time evolution of a dopant atom wave function in an inhomogeneous field and the description of the interaction of two or more dopants in a field.

Dopant atoms binding one electron or hole can be described as a hydrogen atom, where the vacuum values of the dielectric constant and the electron mass are replaced by the appropriate values for the semiconductor. This "scaled hydrogen model" (SHM) provides a reasonable description of the dopant atom's energy levels. Therefore, it is useful to look at existing studies of the Stark effect in the hydrogen atom. Calculation of the shift and splitting of the hydrogen energy levels up to very large electric fields have been carried out by several different methods.[4–6] Within the SHM, these results can be directly translated to dopant atoms in a uniform electric field. However, we found that almost no actual results of such calculations in the (field) range of interest for ASE have been published.

The SHM also offers a manageable way to describe a dopant atom in an inhomogeneous electric field. Recently, several calculations using this framework have been published[7–9] in the context of quantum computing. However, the SHM fails in the explanation of effects where it is essential that the band structure of the semiconductor is taken into account (as an example, see Ref. 10).

Many measurements of the energy levels of dopant atoms in semiconductors (large ensembles) are known, but only a few concerning the effect of a uniform electric field have been reported, presumably because such measurements are much more difficult than, e.g., measurements in a magnetic field or under stress. Among them are spectroscopic measurements of the boron energy levels in silicon subject to electric fields up to 0.15 MV/m.[11] Electron-spin-resonance experiments[12] demonstrated that the electric field couples linearly to the acceptor ground state. The magnitude of the effective electric dipole moment for linear Stark coupling has been estimated as 0.26 D for boron acceptors in silicon ($1\mathrm{D} = 3.3 \times 10^{-30}$ Cm). Photo-ionization measurements have shown a very large electric field effect on the phosphorus ground state in Si,[13] but this was measured in highly doped samples where the interaction between dopants dominates the Stark effect of individual energy levels. Finally, quadratic level shifts have been observed in deep selenium double donors in Si, located in the space charge region of a diode.[14]

In this paper, we will theoretically investigate the effect of a uniform electric field on isolated shallow impurities in silicon. The primary interest for ASE will be in the ground state and possibly the first few excited states. These states are the only ones that are well separated from neighboring levels, and at low temperatures only the ground state is occupied. Therefore, we focus on the lowest energy states of impurities in silicon. First, we derive the shift, splitting, and wave functions of the lowest donor levels in silicon in a small uniform electric field, taking full account of the multiple valley conduction band structure (Sec. II). We briefly outline a similar calculation for acceptors in silicon (Sec. III). The results are useful for applications where a local gate is used to bring a single dopant atom into resonance with a global radiation field (nuclear magnetic resonance, electron spin resonance).

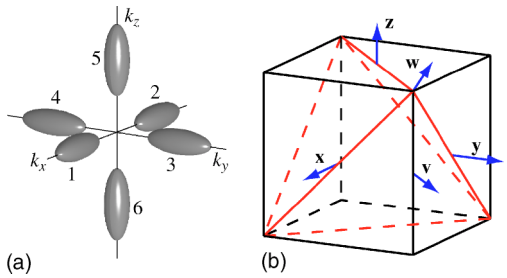

FIG. 1. (Color online) (a) Schematic representation of the conduction band valleys of silicon as constant energy surfaces in k space. The six valleys are labeled by numbers, e.g., 4 represents the $[0\bar{1}0]$ valley. (b) Definition of the coordinate system with respect to the Si-crystal unit cell. We have $\mathbf{x}\|[100]$, $\mathbf{y}\|[010]$, $\mathbf{z}\|[001]$, $\mathbf{v}\|[110]$, and $\mathbf{w}\|[111]$. The orientation of the figure in parts (a) and (b) is the same.

Moreover, they can be used to outline the limitations of the SHM. Second, in Sec. IV we present accurate numerical calculation of the Stark effect in silicon within the SHM, from zero field up to fields that are relevant for atomic scale electronics and quantum computing (several MV/m; see, for instance, Ref. 3). Finally, we conclude by discussing possible extensions and alternatives of our methods which are useful to address issues in ASE (Sec. V).

II. DONORS

A. The donor ground state

Group theory is a powerful tool to derive various properties of dopant wave functions in a semiconductor. In order to provide the necessary background and to fix the notation, we will briefly review some relevant properties of donor levels in silicon (see, e.g., Ref. 15). Degeneracy due to spin is not lifted by an electric field in donors. For simplicity, we will therefore not count those degeneracies in this section.

The conduction band of silicon has six equivalent minima located on the [100] and equivalent axes. These minima are commonly called "valleys" and we label them by the numbers 1 to 6 as shown in Fig. 1(a). The band structure in the vicinity of valley 1, located in k space at $\mathbf{k}_1=(k_0,0,0)$, can be approximated as

$$E = E_0 + \frac{\hbar^2}{2m_\parallel}(k_x - k_0)^2 + \frac{\hbar^2}{2m_\perp}(k_y^2 + k_z^2),$$

where $m_\parallel = 0.98m$ and $m_\perp = 0.19m$ are the electron effective masses and m is the free electron mass. Furthermore, $k_0 = 0.85 \times 2\pi/a$,[16] where a is the size of the silicon unit cell. Similar expressions hold for the remaining five valleys.

From effective mass theory (EMT) it follows that the ground state wave function of the Hamiltonian of an electron bound to a donor can be written as[17]

$$\Psi(\mathbf{r}) = \sum_{\mu=1}^{6} \alpha_\mu F_\mu(\mathbf{r})\varphi_\mu(\mathbf{r}), \tag{1}$$

where the α_μ are numerical coefficients and the $F_\mu(\mathbf{r})$ are envelope wave functions, which are slowly varying on the length scale of a. $F_1(\mathbf{r})=F_2(\mathbf{r})$ satisfy the hydrogenlike Schrödinger equation

$$-\left[\frac{\hbar^2}{2m_\parallel}\frac{\partial^2}{\partial x^2} + \frac{\hbar^2}{2m_\perp}\left(\frac{\partial^2}{\partial y^2} + \frac{\partial^2}{\partial z^2}\right) + \frac{e^2}{4\pi\varepsilon r}\right]F(\mathbf{r}) = EF(\mathbf{r}), \tag{2}$$

and similar equations hold for the remaining F_μ. The $\varphi_\mu(\mathbf{r})$ are Bloch wave functions at the minimum of the valley μ and can be written as $e^{i\mathbf{k}_\mu\cdot\mathbf{r}}u_\mu(\mathbf{r})$, where $u_\mu(\mathbf{r})$ has the periodicity of the silicon crystal lattice. Because for all μ the eigenvalues resulting from Eq. (2) are the same, Eq. (1) shows that the degeneracy of each of these eigenvalues is multiplied by six for the total wave functions $\Psi(\mathbf{r})$. In particular, the ground state solution of Eq. (2) gives rise to a sixfold degenerate donor ground state.

The symmetry group of the conduction band minima [and thus of the Bloch functions $\varphi(\mathbf{r})$] is $C_{\infty v}$ in EMT, which reduces to C_{2v} in the silicon crystal. The envelope wave functions $F(\mathbf{r})$ belong to $D_{\infty h}$. Their products belong to the cross section of both groups, which is C_{2v}. For the 1s-like ($m=0$) ground state function of Eq. (2) $F_\mu(\mathbf{r})$, such a product transforms according to the Γ_1 representation of the valley symmetry group C_{2v}. Because the donor is located at a substitutional site of the tetrahedral silicon lattice, the total wave function has T_d symmetry. Using Frobenius' theorem,[18] it can be shown that the Γ_1 representation of C_{2v} induces the $\Gamma_1+\Gamma_3+\Gamma_5$ representation[19] of T_d. This means that linear combinations of the F_μ(r) can be found that have the correct transformations properties under T_d. Using the notation $\boldsymbol{\alpha} = (\alpha_1, \ldots, \alpha_6)$ [as in Eq. (1)] the reduction to the T_d representations is carried out by

$$\left.\begin{aligned} \boldsymbol{\alpha}_g &= \frac{1}{\sqrt{6}}(1,1,1,1,1,1), \quad \Gamma_1, \\ \left.\begin{aligned} \boldsymbol{\alpha}_r &= \frac{1}{\sqrt{12}}(-1,-1,-1,-1,2,2) \\ \boldsymbol{\alpha}_s &= \frac{1}{2}(1,1,-1,-1,0,0) \end{aligned}\right\}, \quad \Gamma_3, \\ \left.\begin{aligned} \boldsymbol{\alpha}_x &= \frac{1}{\sqrt{2}}(1,-1,0,0,0,0) \\ \boldsymbol{\alpha}_y &= \frac{1}{\sqrt{2}}(0,0,1,-1,0,0) \\ \boldsymbol{\alpha}_z &= \frac{1}{\sqrt{2}}(0,0,0,0,1,-1) \end{aligned}\right\}, \quad \Gamma_5. \end{aligned}\right. \tag{3}$$

Each of the vectors $\boldsymbol{\alpha}$ defines a wave function Ψ through Eq. (1). Here, the basis functions of the two- and three-dimensional representations have been chosen such that Ψ_r and Ψ_s transform under T_d as $3z^2-r^2$ and $\sqrt{3}(x^2-y^2)$, respectively. Similarly, Ψ_x, Ψ_y, and Ψ_z have been chosen such that they transform under T_d as x, y, and z, respectively.

The potential term in the EMT Schrödinger equation (2) is a good approximation only for $r \gtrsim a$, where a is the lattice constant of silicon. For small r, the charge of the nucleus is

TABLE I. Reduction of the site symmetry of an impurity in a uniform electric field in various directions and the resulting reduction of the irreducible representations (Ref. 20).

	Direction		
	⟨100⟩	⟨111⟩	⟨110⟩
	Group		
	$\overline{C}_{2v}$	$\overline{C}_{3v}$	$\overline{C}_{s}$
Γ_1 (T_d)	Γ_1	Γ_1	Γ_1
Γ_2 (T_d)	Γ_3	Γ_2	Γ_2
Γ_3 (T_d)	$\Gamma_1+\Gamma_3$	Γ_3	$\Gamma_1+\Gamma_2$
Γ_4 (T_d)	$\Gamma_2+\Gamma_3+\Gamma_4$	$\Gamma_2+\Gamma_3$	$\Gamma_1+2\Gamma_2$
Γ_5 (T_d)	$\Gamma_1+\Gamma_2+\Gamma_4$	$\Gamma_1+\Gamma_3$	$2\Gamma_1+\Gamma_2$
Γ_6 ($\overline{T}_d$)	Γ_5	Γ_4	Γ_{3+4}
Γ_7 ($\overline{T}_d$)	Γ_5	Γ_4	Γ_{3+4}
Γ_8 ($\overline{T}_d$)	$2\Gamma_5$	$\Gamma_4+\Gamma_{5+6}$	$2\Gamma_{3+4}$

not screened by other electrons and it will attract electrons much more strongly than described by the potential in Eq. (2). Because the symmetry of the potential is not affected, the states are still described by the representations of T_d, but they are no longer degenerate. The Γ_1 state Ψ_g is the only one of the six ground state wave functions that has nonzero electron density at the nucleus ($\mathbf{r}=\mathbf{0}$). Therefore, it has a larger binding energy than predicted by EMT and for most donors in silicon the $1s(\Gamma_1)$ state is the true ground state. This effect is generally called "chemical splitting" (because the size of the effect depends on the donor in question) or "valley-orbit splitting." The remaining states (especially the non-s states) are quite well described by EMT, because the electron density at the nucleus is negligible. As an example, in case of phosphorus in silicon, the $1s(\Gamma_1)$ state (the ground state) has been measured to be located 45.29 meV below the conduction band minimum,[1] while the EMT prediction is 31.27 meV.[21]

B. Symmetry of the donor ground state in an electric field

After this brief review of established knowledge of silicon donors, we return to the main subject of this paper. From purely symmetry based considerations, we can find how the Hilbert subspace spanned by the original six valley wave functions is decomposed by the application of an electric field in a certain direction. The impurities considered in this paper occupy substitutional sites in the silicon lattice and their wave functions transform according to representations of site symmetry group $\overline{T}_d$. The symmetry group of a uniform electric field $\boldsymbol{\mathcal{E}}$ is $C_{\infty v}$. When $\boldsymbol{\mathcal{E}}$ is applied in an arbitrary direction in the silicon crystal, the symmetry group $\overline{T}_d$ of the Hamiltonian reduces to the trivial group C_1. Only when the direction of the field is along one of the main crystallographic directions of the crystal, the result is C_{2v} for $\boldsymbol{\mathcal{E}}\|\langle 100\rangle$, C_{3v} for $\boldsymbol{\mathcal{E}}\|\langle 111\rangle$, and C_s for $\boldsymbol{\mathcal{E}}\|\langle 110\rangle$. The reduction of symmetry can induce a splitting in the original energy levels as shown in Table I. As expected, the electric field does not remove degeneracy due to time-reversal symmetry

TABLE II. By considering the symmetry of the valley wave functions in an electric field, the symmetry of the total wave function they induce can be obtained. The results for the 1s level, without considering valley-orbit splitting, are shown in this table. The direction of $\boldsymbol{\mathcal{E}}$ in the first column is denoted by the vectors defined in Fig. 1(a). The fifth column lists the representations of the appropriate site symmetry group, given in the second column. The basis vectors are given in the notation of Eq. (3).

Direction of $\mathcal{E}$	Site symmetry	Valley	Valley symmetry	Γ(site)	Basis
z	C_{2v}	1, 2, 3, 4	C_1	Γ_1	(1,1,1,1,0,0)
				Γ_2	(1,−1,1,−1,0,0)
				Γ_3	(1,1,−1,−1,0,0)
				Γ_4	(1,−1,−1,1,0,0)
		5	C_{2v}	Γ_1	(0,0,0,0,1,0)
		6	C_{2v}	Γ_1	(0,0,0,0,0,1)
w	C_{3v}	1, 3, 5	C_s	Γ_1	(1,0,1,0,1,0)
				Γ_3	(ω^2,0,ω,0,1,0)
					(ω,0,ω^2,0,1,0)
		2, 3, 6	C_s	Γ_1	(0,1,0,1,0,1)
				Γ_3	(0,ω^2,0,ω,0,1)
					(0,ω,0,ω^2,0,1)
v	C_s	1, 3	C_1	Γ_1	(1,0,1,0,0,0)
				Γ_2	(1,0,−1,0,0,0)
		2, 4	C_1	Γ_1	(0,1,0,1,0,0)
				Γ_2	(0,1,0,−1,0,0)
		5	C_s	Γ_1	(0,0,0,0,1,0)
		6	C_s	Γ_1	(0,0,0,0,0,1)

and therefore all resulting levels are at least twofold degenerate.

To make the connection to the valley wave functions $F_\mu(\mathbf{r})\phi_\mu(\mathbf{r})$, we will now discuss the symmetry of the 1*s* levels in an electric field from another point of view. We start by looking at the individual valley wave functions and subsequently derive which linear combinations form appropriate donor wave functions (using the method of Ref. 22). When a donor impurity in silicon is situated in an electric field along the positive *z* direction, the valleys 5 and 6 keep their C_{2v} symmetry, while the field reduces the symmetry group of the other four valleys to C_1. These four valleys are mixed by the elements of the site symmetry group C_{2v} and are therefore grouped together in the third column of Table II.

In case of a 1*s* state, the valley wave functions belong to the Γ_1 representation of C_{2v} (for valleys 5 and 6) or C_1 (for 1, 2, 3, and 4). This is found by reducing the even $m=0$ representation of $D_{\infty h}$ to C_{2v} and C_1, respectively. By using Frobenius' theorem, it can be deduced that these generate for the impurity wave function the representations Γ_1 and $\Gamma_1+\Gamma_2+\Gamma_3+\Gamma_4$ of C_{2v}, respectively. This is also shown in Table II, together with the (set of) induced wave function(s) spanning the subspace of that representation. In a similar way, we obtained results for the electric field in the other main crystallographic directions. They are also shown in the table.

Due to the valley-orbit splitting (which has been ignored so far) the three irreducible components of the donor ground state are already energetically separated at zero field. Therefore, the basis vectors have to be chosen in such a way that they agree with the zero-field energy splitting of the Γ_1, Γ_3, and Γ_5 levels of T_d.[23] The result for various directions of the electric field is shown in Table III.

C. Shift and splitting in an electric field

Now, we will derive the shift and splitting of the lowest donor levels in an electric field from a perturbation calculation. Results for other levels can be derived using the same method, although (because the level spacing is smaller for higher levels) the range of fields where the perturbation calculation is valid is much smaller.

Although the sixfold degeneracy of the 1*s* levels is lifted by the valley-orbit interaction, the complete manifold is relatively well separated from the higher levels [the separation of the highest $1s(\Gamma_3)$ level to closest exited level $(2p_0)$ is roughly twice as large as the separation between the $1s(\Gamma_1)$ and $1s(\Gamma_3)$ levels]. Therefore, we consider the 1*s* manifold as a whole in a single perturbation calculation, taking only the coupling among the 1*s* levels themselves into account.

The electric field couples to the (induced) dipole moment $\mathbf{D}=e\mathbf{r}$ of the impurity state and gives rise to an additional term in its Hamiltonian $-\boldsymbol{\mathcal{E}}\cdot\mathbf{D}$, reflecting the energy associated with the dipole in the field. By making use of the Wigner-Eckart orthogonality theorem from group theory,[24] it is possible to find the vanishing matrix elements as well as the dependencies between the nonvanishing matrix elements, as they follow from the symmetry of the system. The 1*s* submatrix $[\mathcal{H}]$ of the total Stark Hamiltonian $\mathcal{H}=\mathcal{H}_0+\boldsymbol{\mathcal{E}}\cdot\mathbf{D}$ is given by

$$\begin{pmatrix}
E_1 & 0 & 0 & p_{15}\mathcal{E}_x & p_{15}\mathcal{E}_y & p_{15}\mathcal{E}_z \\
0 & E_3 & 0 & -p_{35}\mathcal{E}_x & -p_{35}\mathcal{E}_y & 2p_{35}\mathcal{E}_z \\
0 & 0 & E_3 & p_{35}\sqrt{3}\mathcal{E}_x & -p_{35}\sqrt{3}\mathcal{E}_y & 0 \\
\overline{p}_{15}\mathcal{E}_x & -\overline{p}_{35}\mathcal{E}_x & \overline{p}_{35}\sqrt{3}\mathcal{E}_x & E_5 & p_5\mathcal{E}_z & p_5\mathcal{E}_y \\
\overline{p}_{15}\mathcal{E}_y & -\overline{p}_{35}\mathcal{E}_y & \overline{p}_{35}\sqrt{3}\mathcal{E}_y & \overline{p}_5\mathcal{E}_z & E_5 & p_5\mathcal{E}_x \\
\overline{p}_{15}\mathcal{E}_z & 2\overline{p}_{35}\mathcal{E}_z & 0 & \overline{p}_5\mathcal{E}_y & \overline{p}_5\mathcal{E}_x & E_5
\end{pmatrix}.$$

The elements of this matrix are given by $[\mathcal{H}]_{ij}=\langle\varphi_i|\mathcal{H}|\varphi_j\rangle$, where the wave functions φ_i are taken from the basis $(\Psi_g,\Psi_r,\Psi_s,\Psi_x,\Psi_y,\Psi_z)$ as defined before. The energies E_1, E_3, and E_5 are the eigenvalues of the unperturbed Hamiltonian $\mathcal{H}_0$, that is, the zero-field energies of the $1s(\Gamma_1)$, $1s(\Gamma_3)$, and $1s(\Gamma_5)$ level, respectively. For phosphorus in silicon, the values are $E_1=-45.59$ meV, $E_3=-32.58$ meV, and $E_5=-33.89$ meV with respect to the conduction band edge.[1] The parameters p_{15}, p_{35}, and p_5 describe the coupling between the 1*s* levels. As can be seen, these are the only three independent parameters describing the coupling between the levels. They can be expressed in terms of integrals over products of wave functions, e.g., $p_{15}=e\langle\Psi_g|x|\Psi_x\rangle$ and $p_5=e\langle\Psi_y|x|\Psi_z\rangle$.

Perturbation theory is invoked by calculating the eigenvalues and eigenvectors of this 6×6 matrix up to second order in $\mathcal{E}$. This yields the 1*s* energy levels and wave functions as a function of electric field for $\boldsymbol{\mathcal{E}}$ along the three main crystallographic directions. The energy levels are presented in the last column of Table III. From Table III it can be seen that the $1s(\Gamma_1)$ ground state experiences an isotropic quadratic shift downward,[25] while for the other levels the behavior depends on the direction of the electric field. In Fig. 2 the results for $\boldsymbol{\mathcal{E}}\|\langle100\rangle$ are plotted schematically.

TABLE III. Reduction of the 1*s* donor energy levels in an electric field. The basis vectors belonging to these states are given [in the notation of Eq. (3)] in the limit $\mathcal{E}\rightarrow 0$ ($\omega=e^{2\pi i/3}$). The eigenvalues (up to second order in $\mathcal{E}$) are the result of the perturbation calculation described in the text.

Field direction	$\mathcal{E}=0$	$\mathcal{E}\neq 0$	Basis vector(s)	Eigenvalue
z	$\Gamma_1(T_d)$	$\Gamma_1(C_{2v})$	$(1,1,1,1,1,1)/\sqrt{6}$	$E_1-\lvert p_{15}\rvert^2/(E_5-E_1)\mathcal{E}^2$
	$\Gamma_3(T_d)$	$\Gamma_1(C_{2v})$	$(1,1,1,1,-2,-2)/\sqrt{12}$	$E_3+\lvert 2p_{35}\rvert^2/(E_3-E_1)\mathcal{E}^2$
		$\Gamma_3(C_{2v})$	$(1,1,-1,1,0,0)/2$	E_3
	$\Gamma_5(T_d)$	$\Gamma_1(C_{2v})$	$(0,0,0,0,1,-1)/\sqrt{2}$	$E_5+[\lvert p_{15}\rvert^2/(E_5-E_1)+\lvert 2p_{35}\rvert^2/(E_3-E_1)]\mathcal{E}^2$
		$\Gamma_2(C_{2v})$	$(1,-1,1,-1,0,0)/\sqrt{2}$	$E_5+\lvert p_5\rvert\mathcal{E}$
		$\Gamma_4(C_{2v})$	$(1,-1,-1,1,0,0)/\sqrt{2}$	$E_5-\lvert p_5\rvert\mathcal{E}$
w	$\Gamma_1(T_d)$	$\Gamma_1(C_{3v})$	$(1,1,1,1,1,1)/\sqrt{6}$	$E_1-\lvert p_{15}\rvert^2/(E_5-E_1)\mathcal{E}^2$
	$\Gamma_3(T_d)$	$\Gamma_3(C_{3v})$	$(\omega^2,\omega^2,\omega,\omega,1,1)/\sqrt{6}$	$E_3+2\lvert p_{35}\rvert^2/(E_3-E_5)\mathcal{E}^2$
			$(\omega,\omega,\omega^2,\omega^2,1,1)/\sqrt{6}$	
	$\Gamma_5(T_d)$	$\Gamma_1(C_{3v})$	$(1,-1,1,-1,1,-1)/\sqrt{6}$	$E_5\pm(2/3)\sqrt{3}\lvert p_5\rvert\mathcal{E}+[\lvert p_{15}\rvert^2/(E_5-E_1)-4\lvert p_{35}\rvert^2/(E_3-E_5)]\mathcal{E}^2$
		$\Gamma_3(C_{3v})$	$(\omega^2,-\omega^2,\omega,-\omega,1,-1)/\sqrt{6}$	$E_5\mp(1/3)\sqrt{3}\lvert p_5\rvert\mathcal{E}$
			$(\omega,-\omega,\omega^2,-\omega^2,1,-1)/\sqrt{6}$	
v	$\Gamma_1(T_d)$	$\Gamma_1(C_s)$	$(1,1,1,1,1,1)/\sqrt{6}$	$E_1-\lvert p_{15}\rvert^2/(E_5-E_1)\mathcal{E}^2$
	$\Gamma_3(T_d)$	$\Gamma_1(C_s)$	$(1,1,1,1,-2,-2)/\sqrt{12}$	$E_3+\lvert p_{35}\rvert^2/(E_3-E_1)\mathcal{E}^2$
		$\Gamma_2(C_s)$	$(1,1,-1,1,0,0)/2$	$E_3+3\lvert p_{35}\rvert^2/(E_3-E_1)\mathcal{E}^2$
	$\Gamma_5(T_d)$	$\Gamma_1(C_s)$	$(0,0,0,0,1,-1)/\sqrt{2}$	$E_5+\lvert p_5\rvert\mathcal{E}-(1/2)[\lvert p_{35}\rvert^2/(E_3-E_1)-\lvert p_{15}\rvert^2/(E_5-E_1)]\mathcal{E}^2$
		$\Gamma_1(C_s)$	$(1,-1,1,-1,0,0)/\sqrt{2}$	$E_5-\lvert p_5\rvert\mathcal{E}-(1/2)[\lvert p_{35}\rvert^2/(E_3-E_1)-\lvert p_{15}\rvert^2/(E_5-E_1)]\mathcal{E}^2$
		$\Gamma_2(C_s)$	$(1,-1,-1,1,0,0)/\sqrt{2}$	$E_5-3\lvert p_{35}\rvert^2/(E_3-E_1)\mathcal{E}^2$

The corresponding eigenvectors were also obtained from this calculation. In the limit $\mathcal{E}\rightarrow 0$ they coincide with the vectors given in Table III, allowing us to label each eigenvalue with the correct representation. These results are directly applicable in the prediction of allowed optical transitions between the various levels.

We discuss the behavior of the three 1*s* states in more detail. The normalized eigenfunctions in an electric field parallel to **z** (again up to second order in $\mathcal{E}$) corresponding to the eigenvalues already given in Table III are

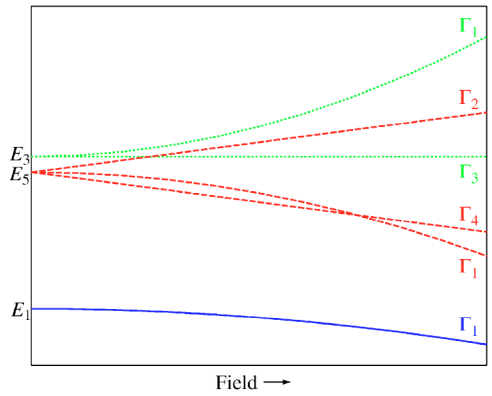

FIG. 2. (Color online) Schematic plot of the 1*s* energy levels as a function of the electric field $\mathcal{E}$. The values of the parameters p_5, p_{15}, and p_{35} have been chosen such that the plot clearly illustrates the qualitative features of the Stark effect in the energy levels.

$$\Phi_g=\left(1-\frac{1}{2}|\beta|^2\mathcal{E}^2\right)\Psi_g+\beta''\mathcal{E}^2\cdot\Psi_r-\bar{\beta}\mathcal{E}\cdot\Psi_z,$$

$$\Phi_r=-\bar{\beta}''\mathcal{E}^2\cdot\Psi_g+\left(1-\frac{1}{2}|\beta'|^2\mathcal{E}^2\right)\Psi_r+\bar{\beta}'\mathcal{E}\cdot\Psi_z,$$

$$\Phi_s=\Psi_s,\quad \Phi_x=\frac{1}{2}\sqrt{2}(\Psi_x+\Psi_y),$$

$$\Phi_y=\frac{1}{2}\sqrt{2}(\Psi_x-\Psi_y),$$

$$\Phi_z=\beta\mathcal{E}\cdot\Psi_g-\beta'\mathcal{E}\cdot\Psi_r+\left[1-\frac{1}{2}(|\beta|^2+|\beta'|^2)\mathcal{E}^2\right]\Psi_z, \tag{4}$$

where

$$\beta=\frac{p_{15}}{E_5-E_1},\quad \beta'=\frac{2p_{35}}{E_3-E_5},\quad \beta''=\bar{\beta}\frac{2p_{35}}{E_3-E_1}.$$

The initial zero-field wave function Ψ_g has the highest spatial symmetry possible in a tetrahedral lattice. To get more insight into the contribution of the six valleys as a function of the applied field, we can write the perturbed ground state wave function Φ_g in the notation of Eq. (3) as

$$(1,1,1,1,1,1) + (0,0,0,0,-\gamma'',\gamma')\mathcal{E} + (-\gamma,-\gamma,-\gamma,-\gamma,-\gamma',-\gamma')\mathcal{E}^2,$$

where

$$\gamma = \frac{1}{2}(|\beta|^2 + \beta''\sqrt{2}), \quad \gamma' = \frac{1}{2}(|\beta|^2 - 2\beta''\sqrt{2}), \gamma'' = \overline{\beta}\sqrt{3}$$

and an overall factor $1/\sqrt{6}$ was omitted. From these expressions, we see that the contribution of the valley in the $-\mathbf{z}$ direction increases linearly with the field, while the contribution of the opposite valley decreases linearly with the field. This reflects the field-induced dipole moment of the ground state.

The results of this calculation could be made quantitative if the values of the parameters p_5, p_{15}, and p_{35} were known. This can be done by evaluating the integrals defining these parameters and using, e.g., the EMT wave functions from Eq. (1). However, due to the strongly oscillating integrants, this is numerically a nontrivial task. Furthermore, the EMT wave functions have a higher symmetry than the lattice, and the value for p_5 obtained in this way is always zero. An estimate for p_5 can be obtained only using more sophisticated approximations for the wave functions. More importantly, the applicability of such results is limited, especially for the 1*s* state, as the effects of valley-orbit interaction are not included in the EMT wave functions.

It is important to note that the energies in Table III and the eigenstates in Eq. (4) are based on symmetry properties only and not on the explicit form of the EMT wave functions. Therefore, these results remain valid, even if valley-orbit interaction and central cell corrections are fully included. Such modifications would influence only the values of the parameters p_5, p_{15}, and p_{35}.

III. ACCEPTORS

Acceptor wave functions can be equally well used for ASE as donors. Recent experiments showing that the coherence time of spins of bound holes is more than 1 ms,[26] even justify the prospective use of acceptor wave functions as qubits. We therefore also briefly outline the properties of silicon acceptors in an electric field, taking the silicon valence band structure into account. The initially threefold degenerate valence band maximum is split by spin-orbit interaction, which causes one of the bands to shift downward by $\sim$43 meV.[1] Due to the spin-orbit interaction, spin is not a good quantum number anymore and the bands must be characterized by the total angular momentum, which is $\frac{3}{2}$ for the upper two bands. Due to the half-valued angular momentum, the Bloch wave function at the valence band maximum transforms according to one of the double-valued representations of $\overline{T_d}$, namely, Γ_8. As a result, the total impurity wave functions transform according to representations of the same group. The ground state wave function, as well as the first few excited levels belong to the Γ_8 representation and they are all fourfold degenerate (including spin).

A. Linear Stark effect

To derive the small-field splitting of acceptors in silicon in an electric field, we use degenerate perturbation theory for each level individually. To that end, the Hamiltonian submatrix $\langle\varphi_i|\mathcal{H}|\varphi_j\rangle$ of the level under consideration must be calculated and diagonalized, where the φ_i form a suitable basis for the subspace of that particular level.

As mentioned before, the components of the electric dipole operator $e\mathbf{r}$ transform according to the rows of the Γ_5 representation of $\overline{T_d}$. Because the antisymmetrized direct products $\{\Gamma_6\times\Gamma_6\}=\{\Gamma_7\times\Gamma_7\}=\Gamma_1$ do not contain Γ_5, the first-order Stark matrix vanishes for levels with Γ_6 or Γ_7 symmetry. Hence, such levels do not experience a linear Stark effect. On the other hand, $\{\Gamma_8\times\Gamma_8\}=\Gamma_1+\Gamma_3+\Gamma_5$ does contain Γ_5, so that a linear Stark effect is possible for a Γ_8 level.[27]

The effective linear Stark Hamiltonian[28] for a Γ_8 level is given by[29]

$$[\mathcal{H}]_8^{\text{lin}} = \frac{2}{\sqrt{3}}p_8(\mathcal{E}_x\{J_y,J_z\} + \mathcal{E}_y\{J_z,J_x\} + \mathcal{E}_z\{J_x,J_y\}),$$

where the parameter p_8 is related to the effective dipole moment of such a state. The J_i $(i=x,y,z)$ are matrices of the components of the angular momentum operator with respect to some convenient basis and $\{A,B\}=\frac{1}{2}(AB+BA)$ is the anticommutator. The eigenvalues of this matrix are given by

$$E_8 \pm |p_8|\mathcal{E},$$

where both eigenvalues occur twice. This is a symmetric splitting of the level, which is independent of the direction of $\boldsymbol{\mathcal{E}}$. Note that p_8 vanishes within the EMT, similar to p_5 before. Estimates of p_8 obtained in literature range from 0.01 D (Ref. 29) to 0.26 D.[12]

B. Quadratic Stark effect

Because $\{\Gamma_6\times\Gamma_6\}=\{\Gamma_7\times\Gamma_7\}=\Gamma_1$, the quadratic effective Stark Hamiltonian for a Γ_6 and Γ_7 level is simply given by

$$\mathcal{H}_{\text{eff,quad}} = a_i\mathcal{E}^2\hat{I},$$

where $\hat{I}$ is the identity matrix and the a_i $(i=6,7)$ are phenomenological parameters, which can be expressed in terms of integrals over wave functions. It follows that the Γ_6 and Γ_7 levels experience an isotropic quadratic shift

$$E_i + a_i\mathcal{E}^2,$$

where E_i is the unperturbed energy of a Γ_i level. The twofold degeneracy due to time-reversal symmetry is obviously not removed by the electric field.

The quadratic part of the effective Hamiltonian for a Γ_8 level, such as the ground state, is given by[29]

$$[\mathcal{H}]_8^{\text{quad}} = a_8\mathcal{E}^2\hat{I} + b_8\left[J_x^2\mathcal{E}_x^2 + J_y^2\mathcal{E}_y^2 + J_z^2\mathcal{E}_z^2 - \frac{1}{3}\mathbf{J}^2\right] + \frac{2}{\sqrt{3}}c_8[\{J_x,J_y\}\mathcal{E}_x\mathcal{E}_y + \{J_y,J_z\}\mathcal{E}_y\mathcal{E}_z + \{J_z,J_x\}\mathcal{E}_z\mathcal{E}_x],$$

where a_8, b_8, and c_8 are again phenomenological parameters. The total Hamiltonian has two distinct eigenvalues

$$a_8\mathcal{E}^2 \pm [p_8^2\mathcal{E}^2 + b_8^2\mathcal{E}^4 + (c_8^2 - 3b_8^2)(\mathcal{E}_y^2\mathcal{E}_z^2 + \mathcal{E}_x^2\mathcal{E}_z^2 + \mathcal{E}_x^2\mathcal{E}_y^2) + 6p_8c_8\mathcal{E}_x\mathcal{E}_y\mathcal{E}_z]^{1/2}, \quad (5)$$

each of which is still doubly degenerate (due to time-reversal symmetry).[30] For $\boldsymbol{\mathcal{E}}\|\langle 100\rangle$ this expression reduces to (up to second order in $\mathcal{E}$)

$$E_8 \pm |p_8|\mathcal{E} + a_8\mathcal{E}^2.$$

For $\boldsymbol{\mathcal{E}}\|\langle 111\rangle$ we find

$$E_8 \pm |p_8|\mathcal{E} + \left(a_8 \pm \frac{1}{3}\sqrt{3}c_8\right)\mathcal{E}^2,$$

and for $\boldsymbol{\mathcal{E}}\|\langle 110\rangle$ we have

$$E_8 \pm |p_8|\mathcal{E} + a_8\mathcal{E}^2,$$

both up to second order in $\mathcal{E}$. The results for $\boldsymbol{\mathcal{E}}\|\langle 100\rangle$ and for $\boldsymbol{\mathcal{E}}\|\langle 110\rangle$ are the same in this approximation, but different in third order.

Obviously, the wave functions of donors and acceptors are very different and this is reflected in their respective electric field behavior. The donor ground state undergoes an isotropic quadratic shift. The acceptor ground state has an isotropic linear splitting, superposed on an anisotropic quadratic shift.

To demonstrate the applicability of these results, we consider White's spectroscopic measurements of boron acceptors in silicon subject to an electric field parallel to the $\langle 110\rangle$ direction.[11] He observes four peaks, which are associated with transitions from the ground state to excited Γ_8 levels (peaks 1, 2, and 3) and a Γ_7 level (peak 4).[31] Level splitting was not observed, most likely due to limited resolution. Indeed, assuming that p_8 for the levels involved has the same order of magnitude as the ground state value (0.26 D; Ref. 12), the expected splitting is only $\sim 1\ \mu$V. However, all peaks do show a quadratic shift, which can directly be linked to the value of a_8 for each of the three excited Γ_8 levels and a_7 for the Γ_7 level.

IV. LARGE ELECTRIC FIELDS IN THE SHM

In this section, we will calculate energy levels of an impurity in a semiconductor as a function of electric field in the range from zero to ~ 5 MV/m. This is done within the scaled hydrogen model, where the band structure of the semiconductor is accounted for by a single effective mass and the dielectric constant only.

For this calculation it is convenient to express all quantities in so-called effective atomic units. For instance, energies are expressed in units of twice the effective ionization energy and length in units of the effective Bohr radius. Conversion of units of the relevant quantities for both vacuum and silicon are given in Table IV.

TABLE IV. Atomic units for some relevant physical quantities in vacuum and in silicon. For silicon the values $\varepsilon_s = 11.4$ and $m^* = 0.26$ (appropriate for electrons) were taken.

Quantity	Unit	Value in vacuum	Value in Si
Energy	2 Ry	27.2 eV	54 meV
Length	a_0	0.053 nm	2.3 nm
Electric field	2 Ry/ea_0	510 GV/m	24 MV/m
Time	$\hbar$/2 Ry	2.4×10^{-17} s	1.2×10^{-14} s

In the past, several algorithms have been described in the literature to calculate electric field dependence of the energy levels of the hydrogen atom. However, very few results in the range of interest for ASE (fields up to ~ 0.1 a.u.; Ref. 3) have been published. Therefore, we found it important to fill this gap by fully presenting the results of our calculation. For this purpose, we used the slightly adapted version of a variational algorithm that yields not only the energy levels, but also their lifetimes.[4]

For completeness, we will very briefly outline the main features of this method. The hydrogen Schrödinger equation (including the electric field) in parabolic coordinates can be separated, which allows for high numerical accuracy without too much computational effort. In order to be able to find the energy positions of the resonances as well as their lifetimes, the complex scaling method was applied.[32] Then, for each coordinate the Hamiltonian (including the electric field) is expanded with respect to a truncated basis of unperturbed wave functions. This can be done analytically. Finally, the energy levels and lifetimes are obtained by tracking (separately for each level) the eigenvalues of this matrix from zero field in small steps to larger fields.

By using the method described above, we calculated the energies of all states with $n=1,2,3$ for $0 \leqslant \mathcal{E} \leqslant 0.2$ a.u. The

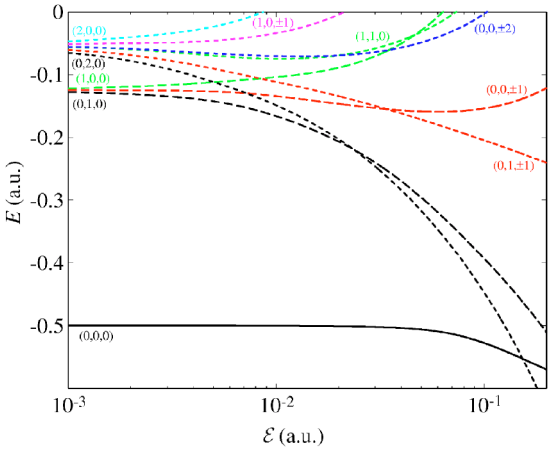

FIG. 3. (Color online) Evolution of the lowest-lying energy levels ($n=1,2,3$) of a hydrogenlike system versus electric field $\mathcal{E}$. For conversion of a.u. to conventional units, see Table IV.

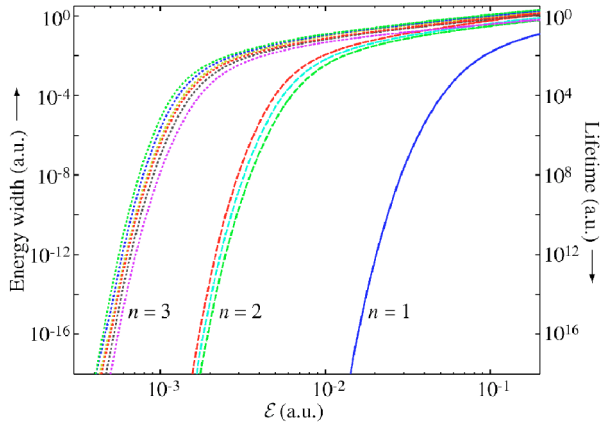

FIG. 4. (Color online) Energy width and lifetime of the lowest-lying energy levels of hydrogen-like systems ($n=1,2,3$) versus electric field $\mathcal{E}$. For conversion of a.u. to conventional units, see Table IV.

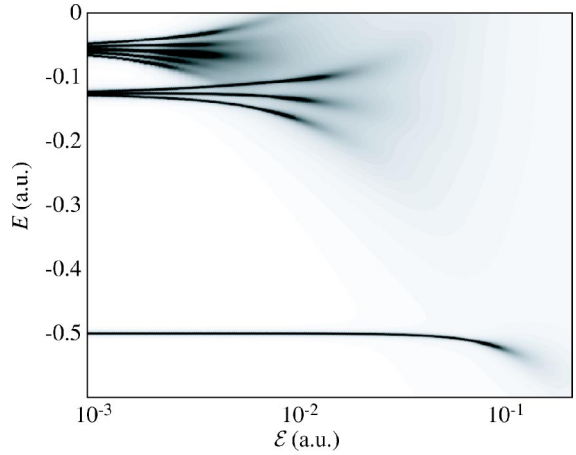

FIG. 5. Map of the energy levels from Fig. 3, converted to Lorentzians using the data of Fig. 4. For conversion of a.u. to conventional units, see Table IV.

results for the energy levels are depicted in Fig. 3. The levels are labeled by parabolic quantum numbers[33] (n_1,n_2,m), which are more suitable for hydrogen in an electric field than the more common spherical quantum numbers (n,l,m). The magnetic quantum number m has the same meaning in both representations. The main quantum number n is related to the parabolic quantum numbers by $n=n_1+n_2+|m|+1$. The electric field lifts all degeneracies except for spin and $(n_1,n_2,\pm m)$. So (including spin) there are both twofold degenerate levels $(m=0)$ and fourfold degenerate levels $(m \neq 0)$.

Figure 3 shows that the ground state $(n=1)$ exhibits a small second-order shift down-ward. The $n=2$ level splits into three levels. Two of them are (for small $\mathcal{E}$) linearly shifting upward and downward. The middle one has no first-order shift, consistent with the well-known results from perturbation theory.[33] Finally, the ninefold degenerate $n=3$ level can be seen to split into six levels. As expected, the effect of the electric field on higher levels is larger, due to their larger spatial extent. At large values of the field, several levels cross each other[34] and some of them show nonmonotonic behavior.

The few results of calculations that can be found in the literature (obtained by different methods) and overlap with our results are in very good agreement, both for the ground state[6] and for the first excited state $(m=1)$.[5]

Not only can the method we used for our calculations be extended to very large fields, but it also has the advantage of yielding the width of the energy levels. The increasing energy width of the hydrogenlike levels in an electric field is the results of the ability of the field to ionize the atom. The finite probability for the carrier to tunnel out of the nucleus' potential well leads to a finite lifetime[36] of the level. In Fig. 4, the evolution of the width of several hydrogen energy levels is depicted. Obviously, the width of all levels is zero at zero field, which is equivalent to an infinitely long lifetime. For any nonzero $\mathcal{E}$, the lifetimes have a finite value, which decreases monotonically with the field. The stronger the binding energy of a level at zero field, the faster the lifetime decreases when the field increases.

In Fig. 5, the results of Figs. 3 and 4 are combined into one "intensity map," where the levels are displayed as normalized Lorentzian line shapes, the width of which is taken from Fig. 4. The figure shows clearly that for the realistic electric field $\mathcal{E}=0.04$ a.u. (about 1 MV/m; see Table IV) the energy width of all levels except the ground state is already larger than or comparable to their binding energy. The ground state lifetime is only 10 ns at that field. We also note that for our purpose it is not very useful to extend the calculation to higher fields, as already at $\mathcal{E}=0.2$ a.u. all levels are very much broadened and strongly overlapping. Although in the case of hydrogen atoms in vacuum such large fields (0.2 a.u. $\sim$ 100 GV/m) are realized only in astronomy, in semiconductors they can be easily achieved under laboratory conditions (0.2 a.u. $\sim$ 5 MV/m).

Though the SHM oversimplifies the band structure, it is in our opinion particularly useful to estimate lifetimes. Figure 4 shows that the lifetimes are primarily a function of the zero-field binding energies. Assuming this is still true when the silicon band structure is included, interpolation of the results can be expected to provide a good first-order approximation of the level's true lifetime. For example, the $n=1$ value in Fig. 4 underestimates the phosphorus donor ground state lifetime, because it is more strongly bound than assumed in EMT.

When the electric field is generated by a small local gate, this gate is usually separated from the semiconductor by a potential barrier that is sufficiently high to prevent tunneling. If the distance of the dopant atom to the barrier is not too small, ionization of the dopant atom can still occur in large fields (and the lifetimes discussed before still apply). However, the charge carrier will not be "lost," but transferred to the potential well created by the biased gate.[8]

V. DISCUSSION AND CONCLUSION

In the preceding sections, we have used two distinct approaches to study the behavior of impurity wave functions in an electric field. The first includes details of the band structure, but is valid only for small fields and is somewhat quali-

tative. From this symmetry-based analysis, we derived the energy level shift and splitting for donors and acceptors in small electric fields, as well as the modification of the donor wave function. Furthermore, the symmetry classification of the resulting levels provides for straightforward prediction of allowed optical transitions.

The second approach, the scaled hydrogen model, is fully quantitative and applicable up to large fields, but neglects most features of the silicon band structure. Still, the SHM offers a manageable and valuable way to describe important phenomena in atomic scale electronics. We presented the energy width and lifetime of the impurity levels in large electric fields, calculated within this framework.

It is possible to combine the two approaches and treat Eq. (2) in a way similar to that presented in Sec. IV. Although this is in principle straightforward, the reduced symmetry and lack of separability will make this approach numerically very involved. Furthermore, it is important to note that the direction of the electric field with respect to the valley axis is not the same for all valleys. As an example, for $\mathcal{E}\|\mathbf{z}$ the energy levels of F_5 and F_6 are affected in a different way from those of the other four F_μ. If the solutions for the various valley wave functions are known, they can be combined into impurity wave functions using the data in Table II.

Although potentially interesting, such an effort is not likely to yield a good description of the dopant's wave function at high electric fields, despite the tremendous increase of necessary computational power. The reason is the omission of valley-orbit interaction, which affects not only the ground state, but also the coupling to excited states. Especially for large fields, the coupling influences the properties of *all* energy levels. It has been shown that intervalley coupling accounts for the splitting of the 1*s* state for P in Si.[37] Inclusion of this effect appears to be a minimum requirement for obtaining accurate quantitative results valid at large fields.

Recently, calculations of a silicon donor in an electric field in the tight binding approach have been presented.[38] This approach seems to be a useful alternative to calculations based on effective mass theory. Given the fact that this method inherently includes the band structure of the semiconductor host, it is striking how similar the results are to calculations based on the SHM.[8] This underlines the power of the SHM in this type of calculation.

In summary, we have calculated the Stark effect of impurities in silicon in two different approaches. Moreover, we discussed the results and the computation methods used in the context of atomic scale electronics and quantum computation.

ACKNOWLEDGMENT

One of us, S.R., wishes to acknowledge the Royal Netherlands Academy of Arts and Sciences for financial support.

*Electronic address: s.rogge@tnw.tudelft.nl

[1] A. Ramdas and S. Rodriguez, Rep. Prog. Phys. **44**, 1297 (1981).
[2] B. E. Kane, Nature (London) **393**, 133 (1998).
[3] B. E. Kane, Fortschr. Phys. **48**, 1023 (2000).
[4] G. Alvarez, R. J. Damburg, and H. J. Silverstone, Phys. Rev. A **44**, 3060 (1991).
[5] F. M. Fernández, Phys. Rev. A **54**, 1206 (1996).
[6] I. A. Ivanov, Phys. Rev. A **56**, 202 (1997).
[7] L. M. Kettle, H.-S. Goan, S. C. Smith, C. J. Wellard, L. C. L. Hollenberg, and C. I. Pakes, Phys. Rev. B **68**, 075317 (2003).
[8] G. D. J. Smit, S. Rogge, J. Caro, and T. M. Klapwijk, Phys. Rev. B **68**, 193302 (2003).
[9] A. Fang, Y. C. Chang, and J. R. Tucker, Phys. Rev. B **66**, 155331 (2002).
[10] B. Koiller, X. Hu, and S. D. Sarma, Phys. Rev. Lett. **88**, 027903 (2002).
[11] J. J. White, Can. J. Phys. **45**, 2695 (1967).
[12] A. Köpf and K. Lassmann, Phys. Rev. Lett. **69**, 1580 (1992).
[13] G. M. Guichar, C. Sebenne, F. Proix, and M. Balkanski, Phys. Rev. B **5**, 422 (1972).
[14] K. Larsson and H. G. Grimmeiss, J. Appl. Phys. **63**, 4524 (1988).
[15] W. Kohn and J. M. Luttinger, Phys. Rev. **98**, 915 (1955).
[16] G. Feher, Phys. Rev. **114**, 1219 (1959).
[17] J. M. Luttinger and W. Kohn, Phys. Rev. **97**, 869 (1955).
[18] M. Hamermesh, *Group Theory and Its Application to Physical Problems* (Addison-Wesley, Reading, MA, 1962).
[19] In literature discussing donors in silicon, it is more common to denote the single-valued representations of T_d by A_1, A_2, E, T_1, and T_2, while for acceptors Γ_i $(i=1,\ldots,5)$ is used. In this paper, we chose to use the Γ_i notation in all cases, following the conventions of Ref. 20 . Moreover, we use the Schönfliess symbols to denote the crystallographic point groups (Ref. 20).
[20] G. F. Koster, J. O. Dimmock, R. G. Wheeler, and H. Satz, *Properties of the Thirty-Two Point Groups* (MIT Press, Cambridge, MA, 1963).
[21] R. A. Faulkner, Phys. Rev. **184**, 713 (1969).
[22] A. K. Ramdas, P. M. Lee, and P. Fisher, Phys. Lett. **7**, 99 (1963).
[23] It is known from group theory that the reduction of a representation containing more than one instance of the same irreducible representation is not uniquely determined.
[24] B. S. Tsukerblat, *Group Theory in Chemistry and Spectroscopy*, Theoretical Chemistry (Academic Press, London, 1994).
[25] In general, the shift of a Γ_1 level cannot have any dependence on the direction of the field.
[26] B. Golding and M. I. Dykman, cond-mat/0309147 (unpublished).
[27] Note that a substitutional site in silicon has no inversion symmetry and therefore no definite parity. This is essential for the occurrence of a linear Stark effect in an isolated level.
[28] In contrast to our treatment of donors, we will use the technique of effective Hamiltonians to derive the matrices for acceptor levels.
[29] G. L. Bir, E. I. Butikov, and G. E. Pikus, J. Phys. Chem. Solids **24**, 1475 (1963).
[30] Note that there is a mistake in the corresponding expression in Ref. 29, where the last term between the square brackets is missing.

[31] At the time of these experiments (1967), the origin of the peaks was not yet resolved.
[32] N. Moiseyev, Phys. Rep. **302**, 211 (1998).
[33] H. A. Bethe and E. E. Salpeter, *Quantum Mechanics of One- and Two-Electron Atoms* (Springer-Verlag, Berlin, 1957).
[34] Levels belonging to the same representation of the spatial symmetry group $C_{\infty v}$ can be seen to cross each other in Fig. 3. This is, however, no violation of the noncrossing rule, since for this specific problem there exists an additional constant of motion that is associated with the separability of the Hamiltonian (Ref. 35).
[35] K. Helfrich, Theor. Chim. Acta **24**, 271 (1972).
[36] This lifetime is solely due to the possibility of ionization and is unrelated to (radiative or nonradiative) transitions from an excited level to a lower state.
[37] A. Balderischi, Phys. Rev. B **1**, 4673 (1970).
[38] A. S. Martins, R. B. Capaz, and B. Koiller, Phys. Rev. B **69**, 085320 (2004).